Integration of artificial neural network and simulated annealing algorithm to optimize deep drawing process

Mohsen Manoochehri & Farhad Kolahan

The International Journal of Advanced Manufacturing Technology

ISSN 0268-3768
Volume 73
Combined 1-4

Int J Adv Manuf Technol (2014)
73:241-249
DOI 10.1007/s00170-014-5788-5

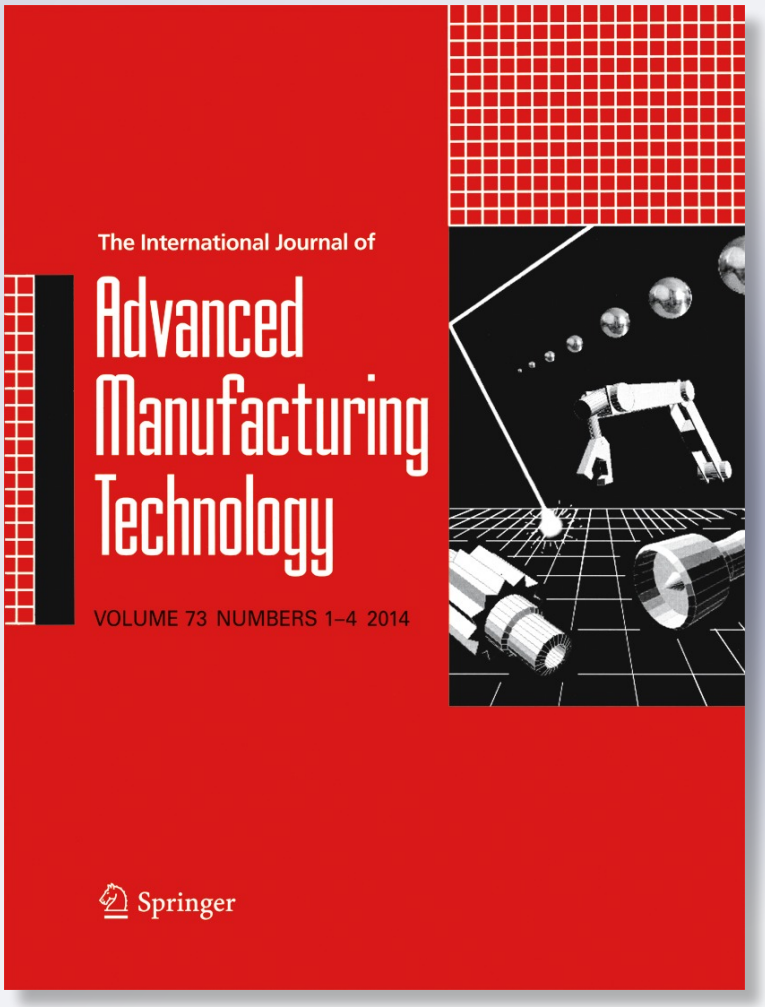

Springer

Int J Adv Manuf Technol (2014) 73:241–249
DOI 10.1007/s00170-014-5788-5

ORIGINAL ARTICLE

Integration of artificial neural network and simulated annealing algorithm to optimize deep drawing process

Mohsen Manoochehri · Farhad Kolahan

Received: 5 December 2012 / Accepted: 14 March 2014 / Published online: 13 April 2014

Abstract Deep drawing is characterized by very complicated deformation affected by the process parameter values including die geometry, blank holder force, material properties, and frictional conditions. The aim of this study is to model and optimize the deep drawing process for stainless steel 304 (SUS304). To achieve the purpose, die radius, punch radius, blank holder force, and frictional conditions are designated as input parameters. Thinning, as one of the major failure modes in deep drawn parts, is considered as the process output parameter. Based on the results of finite element (FE) analysis, an artificial neural network (ANN) has been developed, as a predictor, to relate important process parameters to process output characteristics. The proposed feed forward back propagation ANN is trained and tested with pairs of input/output data obtained from FE analysis. To verify the FE model, the results obtained from the FE model were compared with those of several experimental tests. Afterward, the ANN is integrated into a simulated annealing algorithm to optimize the process parameters. Optimization results indicate that by selecting the proper process parameter settings, uniform wall thickness with minimum thinning can be achieved.

Keywords Deep drawing · Finite element analysis · Optimization · Artificial neural networks

Nomenclature

BHF	Blank holder force
FE	Finite element
σy	Yield stress
σUTS	Ultimate stress
FLDs	Forming limit diagrams
FLSDs	Forming limit stress diagrams
DOE	Design of experiment
ANN	Artificial neural network
R_p	Punch radius
R_d	Die radius
μ_1	Friction coefficient between punch and blank
μ_2	Friction coefficient between die and blank
N	Number of possible design
L	Number of factors
STH_m	Minimum section thickness
BPN	Back propagation network
FEM	Finite element method
MSE	Mean square error
SA	Simulated annealing algorithm
P_r	Probability number
ΔC	Difference between the present and the new objective function value
T_k	Temperature in k-th iteration

M. Manoochehri (✉) · F. Kolahan
Department of Mechanical Engineering, Ferdowsi University of Mashhad, Mashhad, Iran
e-mail: manoochehrimohsen@yahoo.com

F. Kolahan
e-mail: kolahan@um.ac.ir

1 Introduction

Sheet metal forming is a widely used manufacturing process for mass production due to its high speed and low cost. Deep drawing is one of the most common sheet metal forming processes which is widely used for mass production of cup-shaped parts in automobile, petrochemical, and packaging industries [1–4]. Cup drawing is also used as a basic test for sheet metal formability. Figure 1 shows deep drawing tools and the states of forming parts. In this figure, D_o, D_p, c, R_p, and T are the diameter of initial blank, diameter of punch, clearance between punch and die, punch radius, and thickness of blank, respectively.

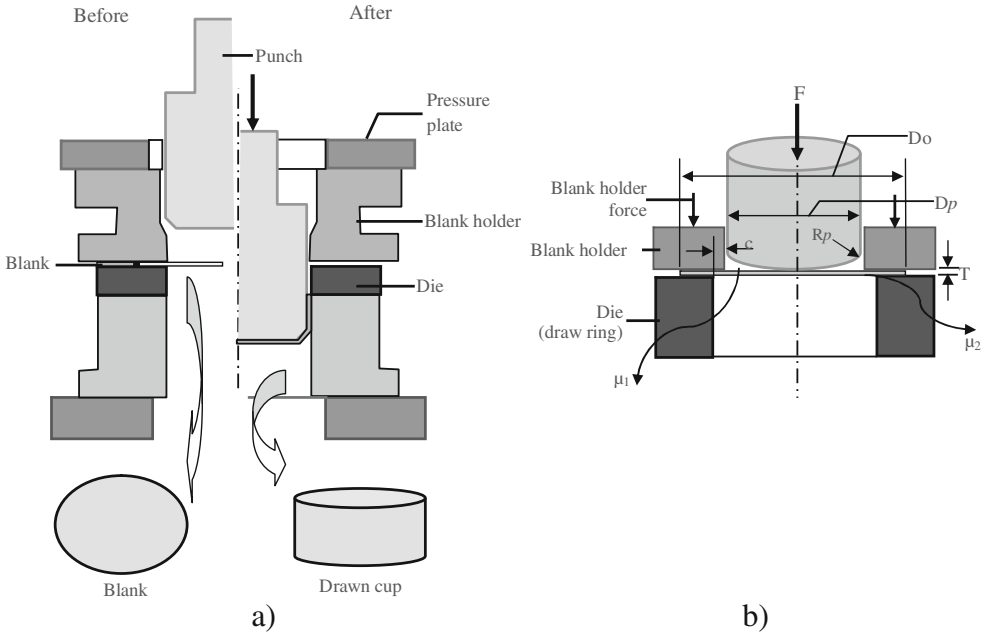

Fig. 1 Deep drawing process. **a** Deep drawing tools. **b** States of forming part

The limits of sheet metal drawability are limited by the onset of process failures: wrinkling, earring, and fracture. Effective parameters on the different types of defects, which may appear in the formed parts, can be divided into three main categories [5]: (1) material properties such as yield stress, work hardening coefficient, anisotropic coefficient, blank dimensions, and thickness of blank; (2) tool properties such as punch radius, die radius, and clearance; and (3) process parameters such as blank holder force (BHF), friction coefficient, type and position of lubricant, strain rate, and pressure.

In order to survive in the daily increasing competitive market, lighter, safer, and cheaper products are required. Subsequently, it is essential to choose the proper drawing parameters which influence the drawing operation. In the past few decades, researchers have focused on the optimization of deep drawing process.

Delamézière et al. [6] optimized the material properties of thin sheets applied in deep drawing. They considered two material parameters: the strain hardening exponent and the average anisotropic coefficient. They defined two objective functions, namely, failure and wrinkling to control the forming defects. Response surface, built on a limited number of evaluations of the objective function, has been employed to optimally determine material properties. Browne and Hillery [2] investigated the variation and effects of punch and die geometry, blank holding pressure, top ram pressure, lubrication, and drawing speed in the deep drawing of C.R.1 steel cups of 0.9 mm thickness. A series of cups were deep drawn using DOE, where a screening experiment was conducted and the desired factors were varied at different levels. Based on their findings, top ram pressure, punch and die profile, lubrication, and position of lubrication are significant factors when measuring the punch load induced. Blank holding pressure, speed, and top ram are the effective parameters on thickness distribution.

Ozek and Bal [7] investigated the effect of die/punch radius and die/blank holder angle on drawability in the deep drawing process. They collected their data using experimental tests with altering variables in five levels. Their results showed that the limit drawing ratio increases with increasing radius of punch and die/blank holder angle.

Padmanabhan et al. [8] studied the significance of three important process parameters, namely, die radius, blank holder force, and friction coefficient on the deep drawing characteristics of a stainless steel axisymmetric cup. They combined the finite element method with Taguchi technique to form a predictive tool to determine the influence of forming process parameters. Their results denote that die radius has the greatest influence on the thickness distribution, followed by the blank holder force and the friction coefficient. Further, they reported that a blank holder force application and local lubrication scheme improved the quality of the formed part. Agrawal et al. [9] performed an attempt to predict the minimum blank holding pressure required to avoid wrinkling in the flange region during axisymmetric deep drawing process.

Singh et al. [10] identified optimum values for die radius, punch radius, friction coefficients, and drawing ratios in deep drawing of St-14 steel plates with initial uniform thickness of 1 mm. Their data have been gathered from 28 experimental tests. Then, artificial neural network (ANN) and genetic algorithm have been used to find the optimal levels of process parameters. Chamekh et al. [11] optimized initial blank shape in a deep drawing process of AISI 304 stainless steel. They built a metamodel by combining the ANN and FEM. Then, the

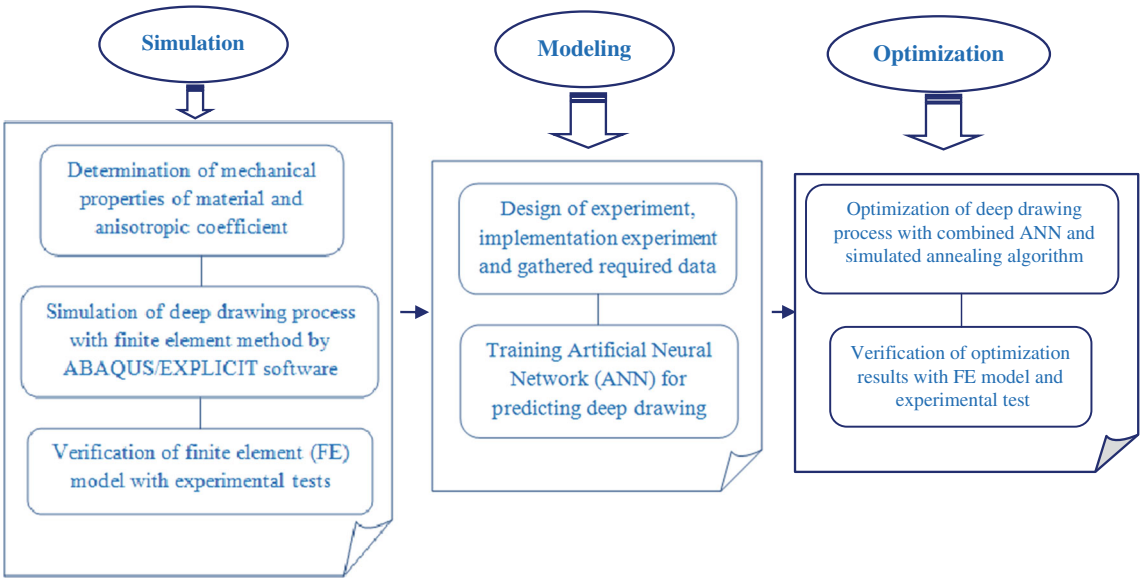

Fig. 2 Flowchart of proposed procedure to modeling and optimization of deep drawing process

metamodel is coupled to an optimization algorithm to determine the initial blank shape for deep drawing of a rectangular cup.

For angular squared deep drawing process, Özek and Ünal [12] have studied the effects of die/blank holder angles, blank holder force, and die/punch diameter on the limit drawing ratio, punch force, and minimum wall thickness of DIN EN 10130-1999 steel sheets. They used a full factorial experimental design for data collection. To model the process and to determine the optimal conditions, they employed regression analysis, signal-to-noise ratio, and analysis of variance (ANOVA). Their results indicate that the deep drawing ratio limits would increase at higher die/blank holder angles and die/punch diameter and that more uniform cup surfaces would be obtained with lower blank holder forces.

A rich body of knowledge in this area can be found in related literature. For instance, Wifi and Abdelmaguid [13] have presented a concise literature review on the optimization techniques used for the single-stage and multistage deep drawing process and identified directions for future research.

In spite of the extensive research work on deep drawing in most current papers, the optimization process is performed based on statistical analysis, which would limit the process variable settings to be chosen solely from a set of pre-specified values.

With regards to this item, the objective of this research is to devise an efficient modeling and optimization procedure for deep drawing process using finite element (FE) modeling, ANN, and simulated annealing (SA) algorithm. The research presented here is twofold. First, an accurate FE model, which can substitute the real deep drawing process, has been developed. Then, to further reduce computational times, an ANN model has been proposed based on the simulation results of D-Optimal matrix. In the second stage, a simulated annealing optimization method has been implemented to optimally determine deep drawing process parameters. The proposed modeling and optimization procedure would treat the process parameters as continuous variables, and hence they can take any values within their feasible ranges.

The important process parameters considered here are die and punch radiuses, BHF, and frictional conditions (friction coefficient between punch–blank, die–blank, and blank holder–blank). Thinning, as a major failure mode or defect encountered in deep drawn parts, has been considered as the process output characteristic. In drawing process, thinning can be defined as the maximum decrease in the blank thickness after drawing compare to its initial value. Figure 2 shows the steps of the proposed procedure to model and to optimize deep drawing process.

2 Material and equipment

In this study, stainless steel 304 (AISI 304) with 0.5 mm thickness has been used for simulation and experimental efforts. Table 1 shows the chemical composition of this material. Mechanical properties and anisotropic coefficients were determined using the results of uniaxial tensile tests. Rolled materials, such as sheet metals, may exhibit anisotropic

Table 1 Chemical composition of SUS 304

Element	Carbon	Manganese	Phosphorus	Sulfur	Silicon	Chromium	Nickel	Nitrogen
Percentage	0.08	2	0.045	0.03	0.75	18–20	8–10.5	0.10

Table 2 Mechanical properties and anisotropic coefficient of SUS 304

Mechanical properties			Anisotropic coefficient		
σ_y (MPa)	σ_{UTS} (MPa)	Young's modulus (GPa)	Angular offset from rolling direction		
			0°	45°	90°
265	573	191.7	0.913	1.120	1.424

mechanical properties, that is, their properties may vary in different directions. To obtain anisotropic coefficients and mechanical properties, tensile tests were performed on three specimens which were cut from the blank in three different directions (0°, 45°, and 90°). Each specimen was prepared according to ASTM B0557 M-02 Standard. The tests were then performed using a Zwick-Z250 tensile test machine. The mechanical properties and the anisotropic coefficient obtained from the uniaxial tests are reported in Table 2. These material properties have been used in the simulation of deep drawing process with the FE method.

Drawing ratio with respect to punch radius (65 mm) and blank diameter (140 mm) is equal to 2.15. A set die has been designed and manufactured to perform the experiments. The set die was mounted on a 60-ton hydraulic press to form parts (Fig. 3). Blank holder force was supplied by eight standard springs with 134 N/mm stiffness. Friction coefficient between the die–blank and punch–blank was obtained by several experiments using a force gauge of 0.01 N resolution.

3 Finite element simulation

In this study, ABAQUS/EXPLICIT software V 6.10 was used to develop a 3D FE model of the deep drawing process for SUS 304 alloy as shown in Fig. 4. Tools (die, punch, and blank holder) were modeled as rigid bodies using R3D4 elements, and the sheet is modeled as a formable body using C3D8R. A surface-to-surface contact model was adopted in which the coulomb friction law has been considered. Three contact pairs, namely, punch–blank, die–blank, and blank holder–blank, were created. Material behavior obtained from the tensile testing experiments and the Hill's anisotropy parameters [14] were incorporated into the FE model to account for the specimen orientation and sheet anisotropy. A constant uniform pressure was applied on the blank holder in Y-direction as the BHF, while the freedom of the blank holder in Y-direction was unfastened.

3.1 Verification of FE model

To validate the developed FE model, the final shape of the drawn parts and the predicted punch loads versus punch strokes were compared with the experimental results under the same process conditions. The comparisons are presented in Fig. 5. With respect to the force–displacement curves, the maximum error of the punch load for the case with wrinkling is less than 9 %. The difference for the parts with no such defect is much less. This is an indication that the FE model is capable of modeling the process under various circumstances

Fig. 3 Hydraulic press and die set used for experiments

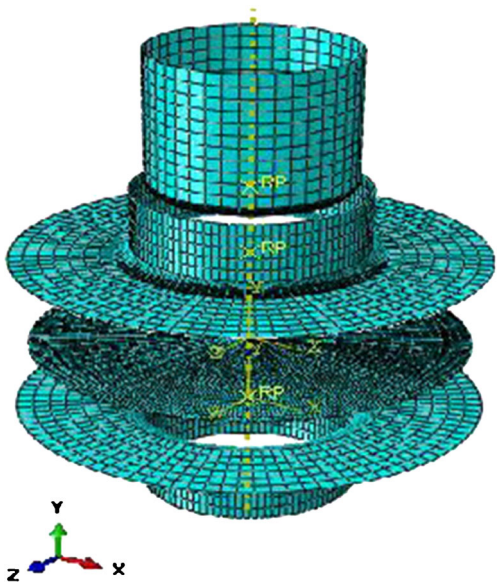

Fig. 4 FE model for the deep drawing of cup-shaped parts

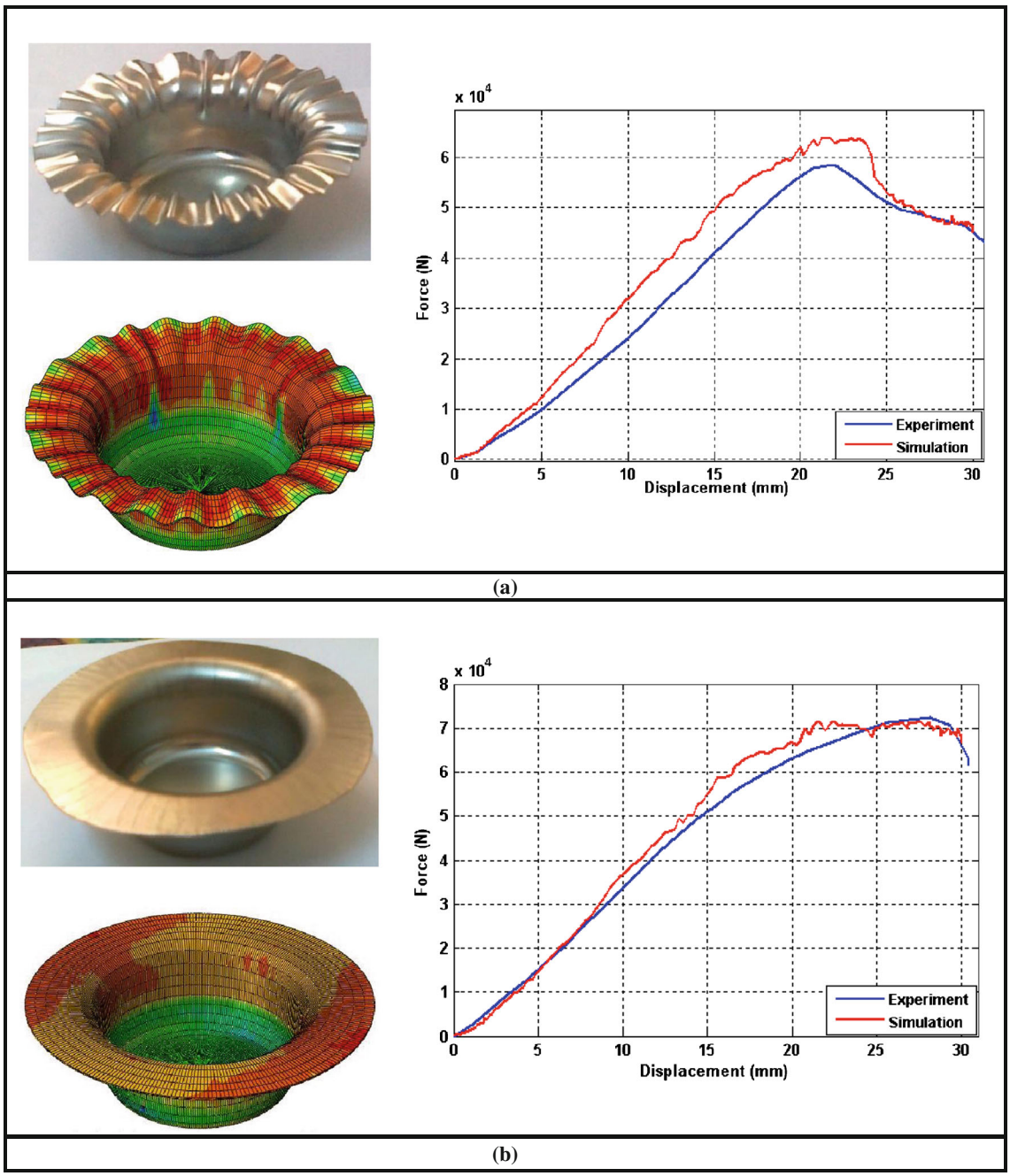

Fig. 5 Simulation and experimental comparisons **a** with wrinkling and **b** without wrinkling

and the simulated formed shapes are consistent with those of experiments.

3.2 Fracture detection in FEM model

In general, fracture can be predicted by: (1) strain-based criteria, such as forming limit diagrams (FLDs) and maximum part thinning; (2) stress-based criteria, using forming limit stress diagrams (FLSDs); and (3) ductile damage criteria, including the Cockroft and Latham criterion [15]. Among these, thinning in the part wall is commonly used in industry to indicate probability of fracture. Usually, a maximum thinning of 25 % thickness is used as the critical fracture criterion

Table 3 Variable parameters with their levels

Levels	BHF (KN)	R_p (mm)	R_d (mm)	μ_1	μ_2
1	5	3	3	0.01	0.01
2	11	5	5	0.1	0.1
3	16	8	8	0.2	0.2
4	22	12	12	–	–

Table 4 Design matrix and output values

Number of experiment	Inputs					Output
	BHF (kN)	R_p (mm)	R_d (mm)	Mu1	Mu2	STH_m[a]
1	5	3	3	0.01	0.01	0.391
2	22	8	3	0.1	0.1	0.374[b]
3	16	12	5	0.1	0.1	0.419
4	22	5	8	0.01	0.01	0.432
5	16	8	12	0.1	0.1	0.444
6	16	12	5	0.01	0.01	0.424
–	–	–	–	–	–	–
–	–	–	–	–	–	–
–	–	–	–	–	–	–
75	11	5	12	0.1	0.01	0.454
76	16	3	3	0.2	0.1	0.374[b]
77	22	12	12	0.1	0.1	0.449
78	5	8	8	0.2	0.2	0.442
79	5	5	8	0.1	0.1	0.431
80	11	5	8	0.01	0.1	0.399
81	22	5	12	0.2	0.1	0.448

[a] Minimum section thickness (mm)

[b] Maximum thinning exceeds from 0.125 mm and hence the drawn part is failed

[16]. Therefore, in the present study, we also have selected wall thinning as the process quality index as well. The maximum allowed thinning of drawn parts for 0.5-mm thickness of blank would be 0.125 mm, which has been used as the acceptance criterion in the analysis.

4 Design of experiment and ANN

One of the main objectives in this research is to predict the product quality under various sets of process parameters. According to the results, the FE model could be used for this purpose. However, it is a time-consuming process as each run of the FE model may take several hours. Therefore, as a more efficient prediction technique, ANN was employed to estimate the process response (thinning) for any given set of process parameters. To gather the required data, a set of simulation runs was performed based on design of experiment (DOE) approach.

Blank holder force (BHF), punch radius (R_p), die radius (R_d), friction coefficient between punch–blank (μ_1), die–blank (μ_2), and holder–blank were considered as input parameters. The ranges of these parameters and their levels are given in Table 3. As shown, the first three parameters are taken to have four levels, while the last two can vary in three levels. Based on the previous researches [17–19], punch and die radius are considered in the range 3–12 mm. All simulation experiments are carried out for the depth of 30 mm.

For a full factorial design, the number of possible designs (N) is $N=L^m$, where L is the number of levels for each factor and m is the number of factors. Thus, a full factorial for input parameters in this study would consist of 576 experiments. To further reduce the number of simulation runs, D-Optimal design of experiments (DOE) has been implemented. In this way, only 81 runs are needed to generate the required data for ANN development. Table 4 illustrates part of the design matrix and measured outputs. In this table, the last column shows the minimum section thickness under each set of input parameters.

4.1 The proposed artificial neural network

ANNs are widely accepted as a tool to simulate complex and ill-defined problems. They are particularly useful in process modeling and have been used in diverse applications such as control, robotics, pattern recognition, forecasting, manufacturing optimization, etc. [20]. Due to the inherent complexity of deep drawing process, the relationships between part quality indexes and process parameters could not be established by any analytical model. On the other hand, the characteristics of

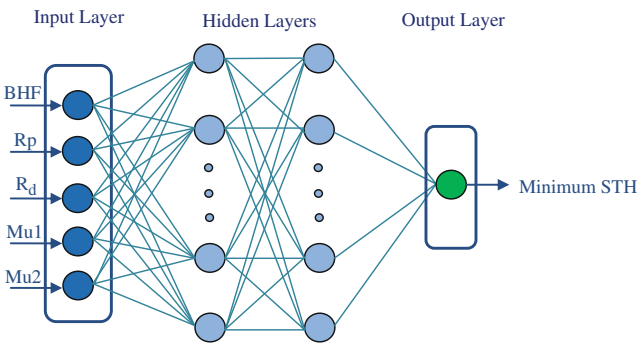

Fig. 6 Schematic illustration of the proposed ANN

Table 5 Optimum parameters

Variables	BHF (kN)	R_p (mm)	R_d (mm)	Mu1	Mu2	STH_m predicted with ANN	STH_m obtained from FEM	STH_m obtained from experiment
Optimum value	8	12	12	0.2	0.01	0.466	0.477	0.43

the ANN technique make it suitable for predicting the thinning in deep drawn parts; therefore, it is employed in this study.

The back propagation network (BPN) is a typical ANN that has been widely used in many research fields. BPNs have hierarchical feed forward network architecture, and the outputs of each layer are sent directly to each neuron in the next layer. This kind of ANN is trained by repeatedly presenting a series of input/output pattern sets to the network. The neural network gradually "learns" the governing relationship in the data set by adjusting the weights between its neurons to minimize the error between the actual and predicted outputs of the training set. A separate set of data called the test set is usually used to evaluate the network's performance. Training is considered completed when the mean squared error (MSE) of the test set reaches a pre-determined value. The MSE formula is:

$$\mathrm{MSE} = \frac{1}{n}\sum_{i=1}^{i=n}(t - t_0)^2 \tag{1}$$

where n is the number of experiments in the test set, t is the predicted thickness, and t_0 is the actual thickness.

The number of neurons for the input layer is equal to the number of process variables. Likewise, the number of neurons at the output layer is specified by the number of measured output responses. Therefore, for the problem under consideration, input and output layers have five and one neuron, respectively. The number of middle (hidden) layers and their corresponding neurons are usually defined through trial runs. Based on the results of several test runs, a four-layer ANN (two hidden layers) with one neuron in the first hidden layer and three neurons in the second hidden layer was found to be the best architecture for the problem under study. The network was trained using resilient back propagation algorithm. Other initial parameters of training algorithm, such as training time and termination criterion, were set according to the defaults of MATLAB software. A schematic illustration of the proposed ANN architecture is presented in Fig. 6.

To train and to test the ANN, 81 sets of input/output samples were randomly divided into two data sets. The 60 set points were assigned to the training set and the remaining 21 set points were used as the testing set. The MSE between the ANN and FEM models was found to be less than 3 %. Therefore, it can be concluded that the proposed ANN is capable to predict the output with high accuracy.

After being trained, the ANN can map the complex and non-linear relation between quality index and input variables of deep drawing process, and hence there is no need to use FE model for this purpose anymore. The developed ANN predictor may now be used in the optimization process using simulated annealing algorithm.

5 Optimization of deep drawing process parameters

The aim of this section is to present an optimization procedure in order to find the process parameter values in such a way that the minimum wall thicknesses of drawn parts are maximized. Simulated annealing (SA) algorithm has been employed to determine the best values of process variables with respect to minimum wall thickness. One of the reasons for selecting SA is because it has fewer parameters compared to other heuristics, such as genetic algorithm (GA), which makes it easier for computer programming.

Simulated annealing is a powerful stochastic technique for obtaining optimum or near-to-optimum solutions to combinatorial and function optimization problems. This algorithm, first proposed by Kirkpatrick et al., is inspired by the thermodynamic process of cooling (annealing) a molten metal to attain the lowest free energy state [21]. A standard SA procedure begins by generating an initial solution at random. At each stage, a small random change is made to the current

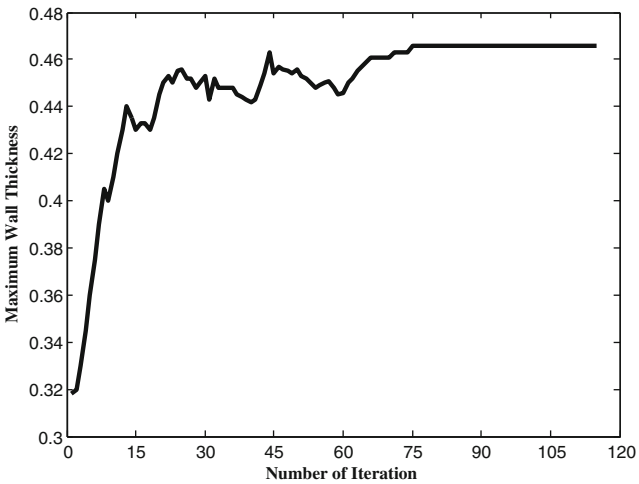

Fig. 7 Simulated annealing performance

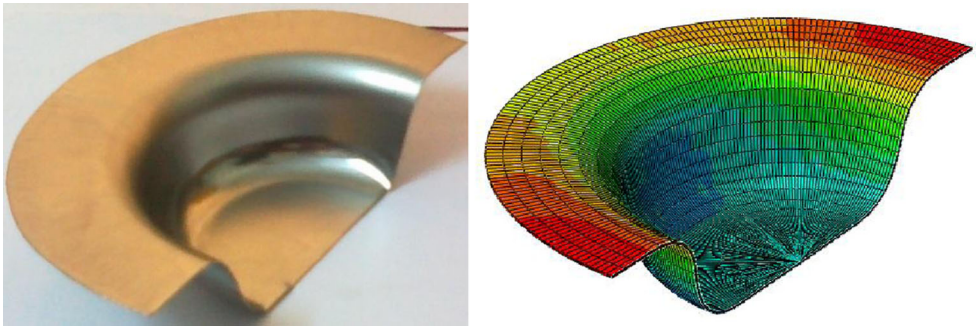

Fig. 8 Formed parts in simulation and experimental test

solution. Then, the objective function value of the new solution is calculated and compared with that of the current solution. A move is then made to the new solution if it has a better value. A non-improving solution is also accepted with the certain probability which is given by $P_r = \exp\left(\frac{-\Delta c}{T_k}\right)$. The acceptance probability of non-improving solutions decreases as the difference in the costs (Δc) increases and as the temperature of the method decreases. As the number of iterations (k) increases, the temperature (T_k) is gradually decreased from a relatively high value to near zero [22].

In order to find the optimum values of the deep drawing parameters, the proposed ANN has been used as the fitness function in SA algorithm. In optimization process, punch and die radius vary from 3 to 12 mm with an increment of 1 mm; BHF is increased from 5 KN with an increment of 1 KN to reach the maximum of 22 KN, and friction coefficients vary according to Table 5.

The algorithm was run for 120 iterations (about 2.0 min). As shown in Fig. 7, the algorithm was converged to the final solution after 75 iterations, and no further improvement was observed thereafter. The optimization results are summarized in Table 5.

Nevertheless, we cannot claim that the results obtained by the proposed SA are global optimum. Computational results merely demonstrate that SA is quite capable of obtaining high-quality solutions (optimal or near-optimal) within reasonable computational times.

To validate the optimization procedure, experimental tests were performed based on the optimum values of process parameters. In addition, FE model was run using the same input values. The last three columns of Table 5 show that the STH_m values were obtained by ANN, FEM, and the experiments, respectively. The error between ANN prediction and FE simulation is less than 2.5 %, while ANN prediction and experimental test show about 8 % error. Figure 8 display drawn parts in simulation and experimental test. It can be concluded that the optimization procedure proposed in this study is capable of achieving the optimal values of the variable parameters with high accuracy.

The proposed procedure for optimization of deep drawing process is efficient and reliable. The optimum set of parameter settings results in a wall thickness better than all 81 other combinations used in data collection.

6 Conclusion

In this study, a combined FE–ANN–SA procedure was proposed to model and to optimize the deep drawing process of SUS304. First, deep drawing process was simulated in ABAQUS software and verified against experimental data. In FE modeling, some of the most important process parameters of deep drawing have been simultaneously considered. This made it possible to develop a model as close to actual process as possible. Next, based on D-Optimal design matrix, a total of 81 simulation runs were performed to gather the required data needed for ANN modeling. Verification tests reveal that the developed ANN is in good agreement with both FEM model and experimental results. Hence, in our future investigations, the FE model and ANN predictor could accurately replace the actual deep drawing process. This would eliminate the need for additional time-consuming and costly experiments. Finally, to determine the optimum values of process parameters, the proposed ANN was used as the fitness function in a simulated annealing algorithm.

Optimization results show that in order to minimize thinning, BHF should be set at 8 KN, and die and punch radius must be at their highest possible levels of 12 mm. Computational results also illustrate that the frictional conditions between blank and die components should not be the same. This is in line with the study previously done in this area [2]. Using optimal parameters, an average improvement of about 14 % in minimum wall thickness can be achieved. The findings of this study show that the combination of ANN, as the process predictor, and SA, as an optimization technique, is quiet efficient in modeling and optimization of deep drawing process.

The approach presented in this work was applied to macro-scale deep drawing process. In the future, the same approach may be used to investigate deep drawing process in micro-scales. It is certainly worthwhile to carry out comparative studies by employing other modeling techniques, such as

regression analysis or response surface method, to model deep drawing process. Another interesting area of research, which calls for further investigation, is the possible implementation of more efficient optimization techniques, such as hybrid GA/SA, for deep drawing optimization. In this case, the results may be compared with those reported in this work.

References

1. Zhang W, Shivpuri R (2009) Probabilistic design of aluminum sheet drawing for reduced risk of wrinkling and fracture. Reliab Eng Syst Saf 94:152–161
2. Browne MT, Hillery MT (2003) Optimising the variables when deep-drawing C.R.1 cups. J Mater Process Technol 136:64–71
3. Wifi AS et al (2007) A review of the optimization techniques applied to the deep drawing process. Proceeding of the 37th International Conference on Computers and Industrial Engineering, October 20–23, 2007, Alexandria
4. Wang L, Lee TC (2005) Controlled strain path forming process with space variant blank holder force using RSM method. J Mater Process Technol 167:447–455
5. Gantar G, Kuzman K (2002) Sensitivity and stability evaluation of the deep drawing process. J Mater Process Technol 125–126:302–308
6. Delamézière A et al (2002) Feasibility in deep drawing: optimization of material properties using response surface. Mécanique Ind 3:93–98
7. Özek C, Bal M (2009) The effect of die/blank holder and punch radiuses on limit drawing ratio in angular deep-drawing dies. Int J Adv Manuf Technol 40:1077–1083
8. Padmanabhan R et al (2007) Influence of process parameters on the deep drawing of stainless steel. Finite Elem Anal Des 43:1062–1067
9. Agrawal A, Reddy NV, Dixit PM (2007) Determination of optimum process parameters for wrinkle free products in deep drawing process. J Mater Process Technol 191:51–54
10. Singh D, Yousefi R, Boroushaki M (2011) Identification of optimum parameters of deep drawing of a cylindrical workpiece using neural network and genetic algorithm. World Acad Sci Eng Technol 5:167–174
11. Chamekh A et al (2010) An optimization strategy based on a metamodel applied for the prediction of the initial blank shape in a deep drawing process. Int J Adv Manuf Technol 50:93–100
12. Özek C, Ünal E (2011) Optimization and modeling of angular deep drawing process for square cups. Mater Manuf Process 26:1117–1125
13. Wifi A, Abdelmaguid T (2012) Towards an optimized process planning of multistage deep drawing: an overview. J Achiev Mater Manuf Eng 55(1):7–17
14. Hill R (1950) The mathematical theory of plasticity. Oxford University Press Inc., New York
15. Sheng ZQ, Jirathearanat S, Altan T (2004) Adaptive FEM simulation for prediction of variable blank holder force in conical cup drawing. Int J Mach Tools Manuf 44:487–494
16. Thomas W (1999) Product tool and process design methodology for deep drawing and stamping of sheet metal parts. Disertation, Ohio State University
17. Colgan M, Monaghan J (2003) Deep drawing process: analysis and experiment. J Mater Process Technol 13:235–241
18. Enzhi G et al (2010) Finite element simulation on the deep drawing of titanium thin-walled surface part. Rare Metals 29:108–111
19. Watiti VB, Labeas GN (2010) Finite element optimization of deep drawing process forming parameters for magnesium alloys. Int J Mater Form 3:97–100
20. Shen C, Wang L, Li Q (2007) Optimization of injection molding process parameters using combination of artificial neural network and genetic algorithm method. J Mater Process Technol 183:412–418
21. Kirkpatrick S, Gelatt CD, Vecchi MP (1983) Optimization by simulated annealing. Science 220:671–680
22. Kolahan F, Sharifinya A (2009) Simultaneous job scheduling and tool replacement based on tool reliability by proposed Tabu-SA algorithm. J Sci Ind Res-JSIR 68:496–504